

---

# NEURAL NETWORKS BASED VARIATIONALLY ENHANCED SAMPLING

---

A PREPRINT

**Luigi Bonati**

Department of Physics, ETH Zurich, 8092 Zurich, Switzerland  
and Institute of Computational Sciences, Università della Svizzera italiana,  
via G. Buffi 13, 6900 Lugano, Switzerland

**Yue-Yu Zhang**

Department of Chemistry and Applied Biosciences, ETH Zurich, 8092 Zurich, Switzerland  
and Institute of Computational Sciences, Università della Svizzera italiana,  
via G. Buffi 13, 6900 Lugano, Switzerland

**Michele Parrinello**

Department of Chemistry and Applied Biosciences, ETH Zurich, 8092 Zurich, Switzerland,  
Institute of Computational Sciences, Università della Svizzera italiana,  
via G. Buffi 13, 6900 Lugano, Switzerland,  
and Italian Institute of Technology, Via Morego 30, 16163 Genova, Italy

May 18, 2022

## ABSTRACT

Sampling complex free energy surfaces is one of the challenges of modern atomistic simulation methods. The presence of kinetic bottlenecks in such surfaces often renders a direct approach useless. A popular strategy is to identify a small number of key collective variables and to introduce a bias that is able to favor their fluctuations in order to accelerate sampling. Here we propose to use machine-learning techniques in conjunction with the recent variationally enhanced method [Valsson and Parrinello, *Physical Review Letters* 2014] to determine such potential. This is achieved by expressing the bias as a neural network. The parameter are determined in a reinforcement learning scheme aimed at minimizing the variationally enhanced sampling functional. This required the development of a new and more efficient minimization technique. The expressivity of neural networks allows accelerating sampling in systems with rapidly varying free energy surfaces, removing boundary effects artifacts, and making one more step towards being able to handle several collective variables.

**Keywords** Molecular dynamics | Enhanced sampling | Machine learning

Machine learning (ML) is changing the way in which modern science is conducted. Atomistic based computer simulations are no exceptions. Since the pioneering work of Behler and Parrinello [1] neural networks or Gaussian processes are now almost routinely used to generate accurate potentials. More recently ML methods have been used to accelerate sampling, a crucial issue in molecular dynamics (MD) simulations, where standard methods allow only a very restricted range of time scales to be explored. An important family of enhanced sampling methods is based on the identifications of suitable collective variables (CVs) which are connected to the slowest relaxation modes of the system [2]. Sampling is then enhanced by constructing an external bias potential  $V(\mathbf{s})$  which depends on the chosen collective variables  $\mathbf{s}$ . In this context machine learning has been applied in order to identify appropriate CVs [3, 4, 5, 6, 7] and to build new methodologies [8, 9, 10, 11, 12]. From these early experiences it is also clear that ML applications can in turn profit from enhanced sampling [13].

Here we shall focus on a relatively new method, called Variationally Enhanced Sampling (VES) [14]. In VES the bias is determined by minimizing a functional  $\Omega = \Omega[V(\mathbf{s})]$ . This functional is closely related to a Kullback Leibler divergence [15]. The bias that minimizes  $\Omega$  is such that the probability distribution of  $\mathbf{s}$  in the biased ensemble  $P_V(\mathbf{s})$  is equal to a pre-assigned target distribution  $p(\mathbf{s})$ . The method has shown to be flexible [16, 17] and has a great potential also for applications different from enhanced sampling. Examples of these heterodox applications are the estimation of the parameters of Ginzburg-Landau free energy models [15], the calculation of critical indexes in second order phase transitions [18], and the sampling of multithermal-multibaric ensembles [19].

Although different approaches have been suggested [20, 21], the way in which VES is normally used is to expand  $V(\mathbf{s})$  in a linear combination of orthonormal polynomials, and use the expansion coefficients as variational parameters. In spite of its many successes, VES is not without problems. The choice of the basis set is often a matter of computational expediency and not grounded on physical motivations. Representing sharp features in the VES may require many terms in the basis set expansion. The number of variational parameters scales exponentially with the number of CVs and can become unmanageably large. Finally non optimal CVs may lead to very slow convergence.

In this paper we use the expressivity [22] of neural networks (NN) to represent the bias potential and a stochastic steepest descent framework for the determination of the NN parameters. In so doing we have developed a more efficient stochastic optimization scheme that can also be profitably applied to more conventional VES applications.

## Neural network based VES

Before illustrating our method, we recall some ideas of CV-based enhanced sampling methods and particularly VES.

### Collective variables

It is often possible to reduce the description of the system to a restricted number of collective variables  $\mathbf{s} = \mathbf{s}(\mathbf{R})$ , functions of the atomic coordinates  $\mathbf{R}$ , whose fluctuations are critical for the process of interest to occur. We consider the equilibrium probability distribution of these CVs as:

$$P(\mathbf{s}) = \int d\mathbf{R} \frac{e^{-\beta U(\mathbf{R})}}{Z} \delta(\mathbf{s} - \mathbf{s}(\mathbf{R})) \quad (1)$$

where  $Z$  is the partition function of the potential energy  $U(\mathbf{R})$ , and  $\beta = (k_B T)^{-1}$  is the inverse temperature. We can define the associated free energy surface (FES) as the logarithm of this distribution:

$$F(\mathbf{s}) = -\frac{1}{\beta} \log P(\mathbf{s}). \quad (2)$$

Then an external bias is built as a function of the chosen CVs in order to enhance sampling. In the umbrella sampling method [23] this bias is static, while in Metadynamics [24] it is iteratively built as a sum of repulsive Gaussians centered on the points already visited.

### The variational principle

In VES a functional of the bias potential is introduced:

$$\Omega[V] = \frac{1}{\beta} \log \frac{\int d\mathbf{s} e^{-\beta(F(\mathbf{s})+V(\mathbf{s}))}}{\int d\mathbf{s} e^{-\beta F(\mathbf{s})}} + \int d\mathbf{s} p(\mathbf{s}) V(\mathbf{s}) \quad (3)$$

where  $p(\mathbf{s})$  is a chosen probability distribution which we call target distribution. The functional  $\Omega$  is convex [14] and the bias that minimizes it is related to the free energy by the simple relation:

$$F(\mathbf{s}) = -V(\mathbf{s}) - \frac{1}{\beta} \log p(\mathbf{s}) \quad (4)$$

At the minimum the distribution of the CVs in the biased ensemble is equal to the target distribution:

$$p_V(\mathbf{s}) = p(\mathbf{s}) \quad (5)$$

where  $p_V(\mathbf{s})$  is defined as:

$$p_V(\mathbf{s}) = \frac{e^{-\beta(F(\mathbf{s})+V(\mathbf{s}))}}{\int d\mathbf{s} e^{-\beta(F(\mathbf{s})+V(\mathbf{s}))}} \quad (6)$$

In other words,  $p(\mathbf{s})$  is the distribution the CVs will follow when minimizing the functional.

## The target distribution

In VES an important role is played by the target distribution  $p(\mathbf{s})$ . A careful choice of  $p(\mathbf{s})$  may focus sampling in relevant regions of the CVs space and in general accelerate convergence [25]. This freedom has been taken advantage of in the so called well-tempered VES [16]. In this variant, one takes inspiration from well-tempered metadynamics [26] and targets the distribution:

$$p(\mathbf{s}) = \frac{e^{-\beta F(\mathbf{s})/\gamma}}{\int d\mathbf{s} e^{-\beta F(\mathbf{s})/\gamma}} \propto [P(\mathbf{s})]^{1/\gamma} \quad (7)$$

where  $P(\mathbf{s})$  is the distribution in the unbiased system and  $\gamma > 1$  is a parameter that regulates the amplitude of the  $\mathbf{s}$  fluctuations. Since at the beginning of the simulation  $F(\mathbf{s})$  is not known,  $p(\mathbf{s})$  is determined in a self-consistent way. Thus also the target evolves during the optimization procedure. In this work we update the target distribution every iteration, although less frequent updates are also possible. This choice of  $p(\mathbf{s})$  has proven to be highly efficient [16].

## Neural network representation of the bias

The standard practice of VES has been so far of expanding linearly  $V(\mathbf{s})$  on a set of basis functions and use the expansion coefficients as variational parameters. Here this procedure is circumvented as the bias is expressed as a deep neural network as shown in figure 1. We call this variant DEEP-VES. The input of the network are the chosen CVs and this information is propagated to the next layers trough a linear combination followed by the application of a non-linear function  $H$  [22]:

$$\mathbf{x}^{l+1} = H(\mathbf{w}^{l+1}\mathbf{x}^l + \mathbf{b}^{l+1}) \quad (8)$$

Here the non linear activation function is taken to be a rectified linear unit. In the last layer only a linear combination is done, and the output of the network is the bias potential.

We are employing NN since they are smooth interpolators: the NN representation ensures that the bias is continuous and differentiable. The external force acting on the  $i$ -th atom can be then recovered as:

$$\mathbf{F}_i = -\nabla_{\mathbf{R}_i} V = -\sum_{j=1}^n \frac{\partial V}{\partial s_j} \nabla_{\mathbf{R}_i} s_j \quad (9)$$

where the first term is efficiently computed via back-propagation. The coefficients  $\{w^i\}$  and  $\{b^i\}$  that we lump in a single vector  $\mathbf{w}$  will be our variational coefficients. With this representation of the bias the functional  $\Omega[V]$  becomes a function of the parameters  $\mathbf{w}$ . Care must be taken to preserve the symmetry of the CVs, such as the periodicity. In order to accelerate convergence we also standardize the input to have mean zero and variance one [27].

$$\mathbf{x}^i = L^i(\mathbf{x}^{i-1}) = H(\mathbf{w}^i\mathbf{x}^{i-1} + \mathbf{b}^i) \quad (10)$$

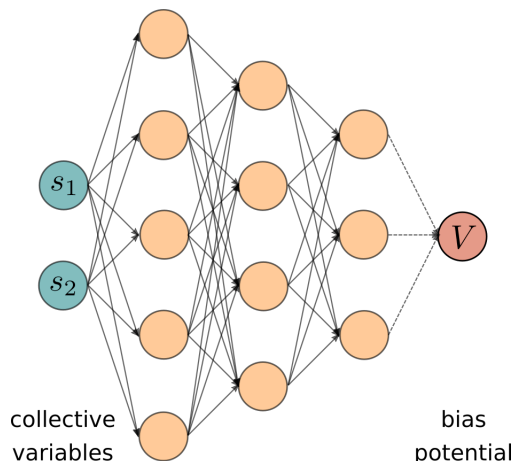


Figure 1: Neural network representation of the bias. The inputs are the chosen collective variables, whose values are propagated across the network in order to get the bias. The parameters are optimized according to the variational principle of eq. 3.

## The optimization scheme

As in all neural network applications, training plays a crucial role. We shall evolve the parameters  $\mathbf{w}$  following the direction of the  $\Omega$  derivatives:

$$\frac{\partial \Omega}{\partial \mathbf{w}} = - \left\langle \frac{\partial V}{\partial \mathbf{w}} \right\rangle_V + \left\langle \frac{\partial V}{\partial \mathbf{w}} \right\rangle_p \quad (11)$$

where the first averages are performed over the system biased by  $V(\mathbf{s})$  and the second over the target distribution  $p(\mathbf{s})$ . Since the calculation of the first term and sometimes also of the second [25] requires performing statistical averages, a stochastic optimization method is necessary. In standard VES applications the method of choice has so far been the one of Bach and Moulines [28], that allows reaching with high accuracy the minimum, provided that the CVs are of good quality. Applying the same algorithm to NNs is rather complex. Therefore we espouse the prevailing attitude in the neural networks community. Namely we do not aim at reaching the minimum but rather to determine a value of the bias  $V_s(s)$  that is close enough to the optimum value to be useful. In the present context this means that a run biased by  $V_s(s)$  can be used to compute the Boltzmann equilibrium averages from the well known umbrella sampling-like formula:

$$\langle O(\mathbf{R}) \rangle = \frac{\langle O(\mathbf{R}) e^{\beta V_s(s(\mathbf{R}))} \rangle_{V_s}}{\langle e^{\beta V_s(s(\mathbf{R}))} \rangle_{V_s}}. \quad (12)$$

In order to measure the progression of the minimization towards eq. 5 we monitor at iteration step  $n$  an approximate Kullback-Leibler (KL) divergence between the running estimates of the biased probability  $p_V^{(n)}(s)$  and the target  $p^{(n)}(s)$ :

$$D_{KL}^{(n)}(p_V \parallel p) = \sum_{\mathbf{s}} p_V^{(n)}(\mathbf{s}) \log \frac{p_V^{(n)}(\mathbf{s})}{p^{(n)}(\mathbf{s})} \quad (13)$$

These quantities are estimated as exponentially decaying averages. In such a way only a limited number of configurations contribute to the running KL divergence.

The simulation is thus divided into three parts. In the first one the ADAM optimizer [29] is used, until a preassigned threshold value  $\epsilon$  for the distance  $D_{KL}(p_V \parallel p)$  is reached. From then on the learning rate is exponentially brought to zero provided that  $D_{KL}$  remains below  $\epsilon$ . From this point on, the network is no longer updated and statistics is accumulated using eq. 12. The longer the second part, the better the bias potential  $V_s$ , and the shorter phase three need to be. Faster decay times instead need to be followed by longer statistics accumulation runs. However in judging the relative merits of these strategies it must be taken into account that the third phase in which the bias is kept constant involves a minor numbers of operations and it is therefore much faster.

## Results

### Wolfe-Quapp potential

We first focus on a toy-model, namely the two-dimensional Wolfe-Quapp potential, rotated as in ref. [21]. This is shown in figure 2a. The reason behind this choice is that the dominant fluctuations that lead from one state to the other are in an oblique direction with respect to  $x$  and  $y$ . We choose on purpose to use only  $x$  as CV to exemplify the case of a sub-optimal CV. This is representative of what happens in the practice when, more often than not, some slow degrees of freedom are not accounted for [21].

We use a three layer neural network with [48,24,12] nodes, resulting in 1585 variational parameters. The network is updated every 500 steps, where the gradients are estimated by sampling. The KL divergence between the biased and the target distribution is computed with an exponential decaying average with a time constant of  $5 \cdot 10^4$  iterations. The threshold  $\epsilon$  is set to 0.5 and the learning rate decay time to  $5 \cdot 10^3$  iterations. The results are robust with respect to the choice of these parameters, see the Supporting Information (SI).

In the upper right panel (figure 2b) we show the evolution of the CV as a function of the number of iterations. At the beginning the bias changes very rapidly with large fluctuations that help exploring the configuration space. It should be noted that the combination of a sub-optimal CV and a rapidly varying potential might lead the system to pathways different from the lowest energy one. For this reason it is important to slow down the learning of the bias as soon as the KL divergence decreases and stays below the threshold value. The learning rate is exponentially lowered until it

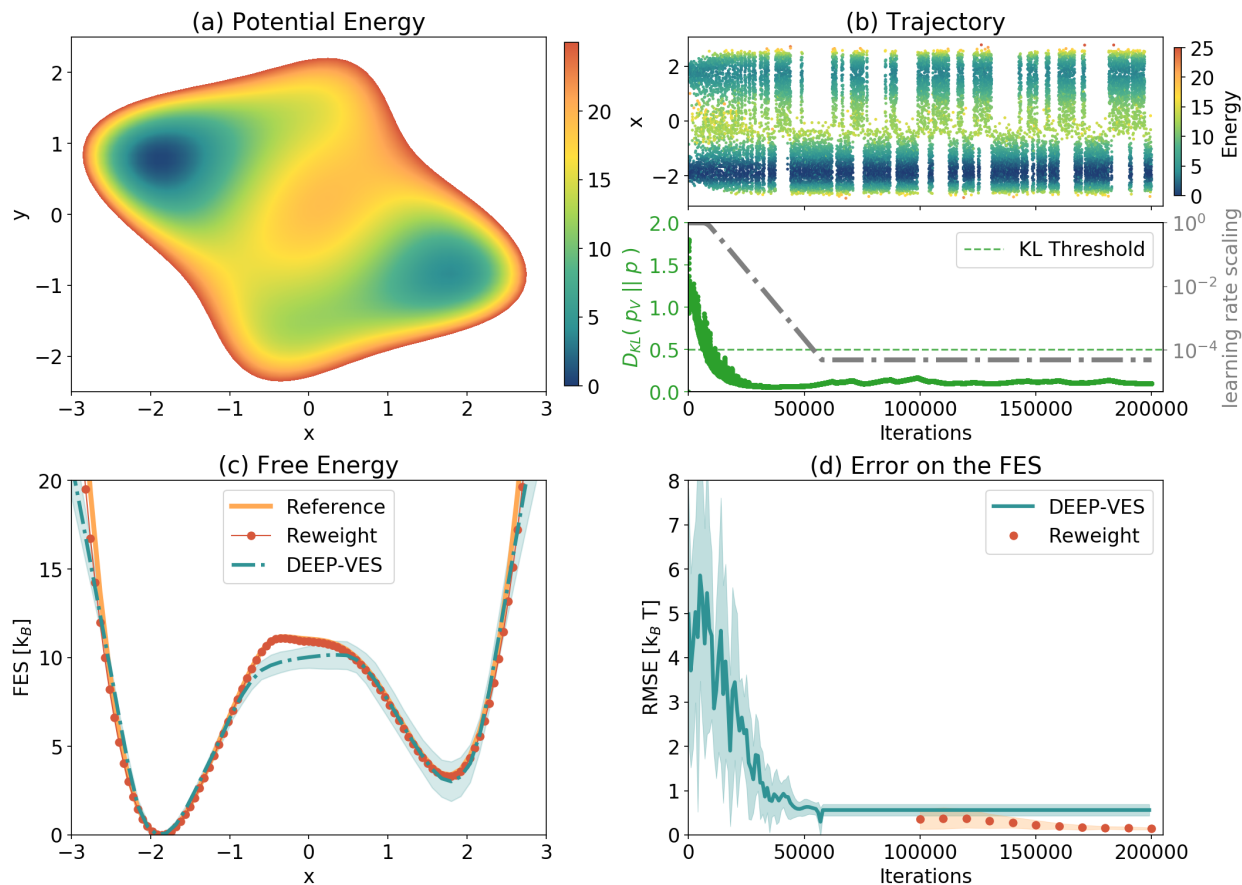


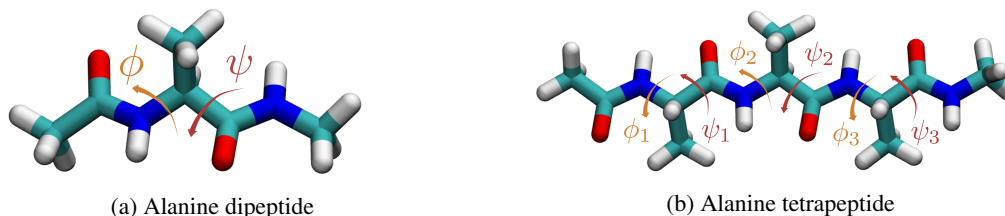
Figure 2: Results for the 2D model. (a) Potential energy surface of the model. (b) Upper panel: CV evolution as a function of the number of iterations. The points are colored according to their energy value. Lower panel: evolution of the KL divergence between the bias and the target distribution (green) and learning rate scaling factor (grey). When the KL divergence is lowered below the threshold value the learning rate is decreased exponentially until it is practically zero. (c) Free energy profiles obtained from the neural network and with the reweighting procedure, compared with the reference obtained by integrating the model. For the DEEP-VES curve also an estimate of the error is given by averaging the results of 8 different simulations. The lack of accuracy on the left shoulder is a consequence of the combination of sub-optimal character of the chosen variable and the strength of the bias, which creates new pathways other than the one of minimum energy. This artifacts are removed by performing the reweight with the static bias potential  $V_s$ . (d) Root mean square error (RMSE) on the FES computed in the regions of  $10 k_B T$  from the reference minimum.

is practically zero. When this limit is reached the frequency of transitions becomes lower, reflecting the sub-optimal character of the CV [21], as can be seen in fig. 2b.

Although the bias itself is not yet fully converged, still the main features of the FES are captured by  $V_s(\mathbf{s})$  (fig. 2c). This is ensured by the fact that while decreasing the learning rate the running estimate of the KL divergence must stay below the threshold  $\epsilon$ , otherwise the optimization proceeds with a constant learning rate. This means that the final potential will be able to efficiently promote transitions between the metastable states. The successive static reweighting refines the FES and leads to a very accurate result (fig. 2d), removing also the artifacts caused in the first part by the rapidly varying potential.

## Alanine dipeptide and tetrapeptide

As a second example we consider the case of two small peptides, Alanine Dipeptide and Alanine Tetrapeptide in vacuum, which are often used as a benchmark of enhanced sampling methods. We will refer to them as Ala2 and Ala4 respectively. Their conformations can be described in terms of the Ramachandran dihedral angles  $\phi_i$  and  $\psi_i$ , where the first have been identified to be the ones connected to the slowest kinetic processes. The smaller Ala2 has only one pair of such dihedral angles, which we will denote as  $\{\phi, \psi\}$ , while Ala4 has three pairs of backbone angles denoted by  $\{\phi_i, \psi_i\}$  with  $i = 1, 2, 3$ .



We want to show here the usefulness of the flexibility given by the NN representation of the bias for different systems. For this purpose we use the same architecture and optimization scheme as in the previous example. We only decrease the decay time of the learning rate in the second phase to  $10^3$  iterations, since  $\phi$  is known to be a good CV. The simulation of Ala2 is carried out by biasing the two angles  $\{\phi, \psi\}$ , while for Ala4 we consider three angles  $\{\phi_1, \phi_2, \phi_3\}$ . In order to enforce the periodicity on the representation of the bias potential, the angles are first transformed in their sines and cosines:  $\{\phi, \psi\} \rightarrow \{\cos(\phi), \sin(\phi), \cos(\psi), \sin(\psi)\}$ .

The simulation of Ala2 reached the KL divergence threshold after 3 ns, and from there the learning rate was exponentially decreased. The NN bias was no longer updated after 12 ns. At variance with the first example, when the learning is slowed down and even when it is stopped the transition rate is not affected: this is a signal that our set of CVs is good (see SI). In figure 4 we show the free energy profiles obtained from the NN bias following eq. 4 and the one recovered with the reweighting procedure of eq. 12. We compute the root mean square error (RMSE) on the FES up to 20kJ/mol as in ref. [16]. The errors are 1.5 and 0.45 kJ/mol, corresponding to 0.6 and 0.2  $k_B T$ , both well below the threshold of chemical accuracy.

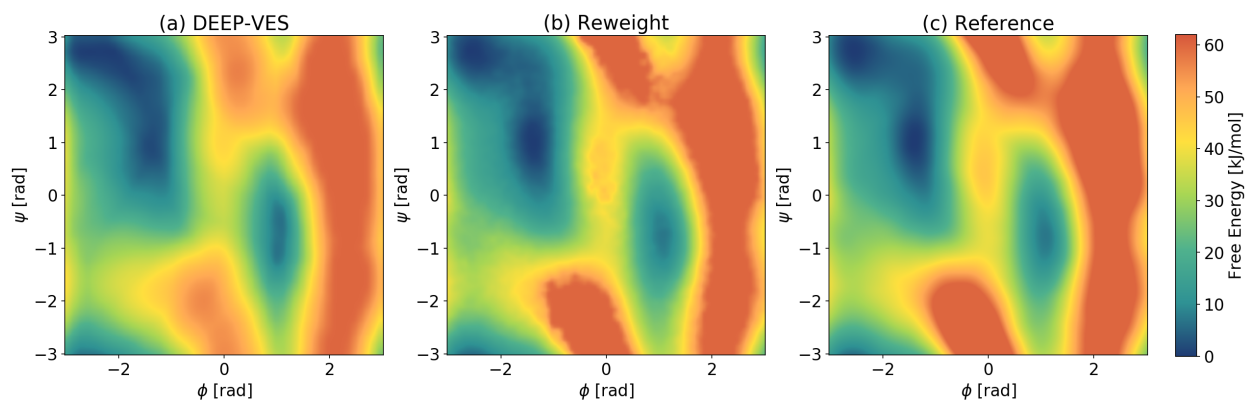


Figure 4: Alanine Dipeptide free energy results. (a) DEEP-VES representation of the bias. (b) FES profile obtained with reweighting. (c) Reference from a 100 ns meta dynamics simulation. The main features of the FES are captured by the the neural network, which allow for an efficient enhanced sampling of the conformations space. Finer details can be easily recovered with the reweighting procedure.

We report also the results for Ala4, biasing along the three dihedrals  $\{\phi_i\}$ . In this case the learning rate start to decrease around 10 ns until stopped at around 20 ns. In figure 5 we report the free energy profiles obtained with the reweighting. The comparison with their reference FES is reported in the SI.

## Silicon crystallization

In the last example the phase transition of silicon from liquid to solid at ambient pressure was studied. This is a complex phenomenon, characterized by a very high barrier of around  $80 k_B T$ , and several CVs have been proposed to enhance

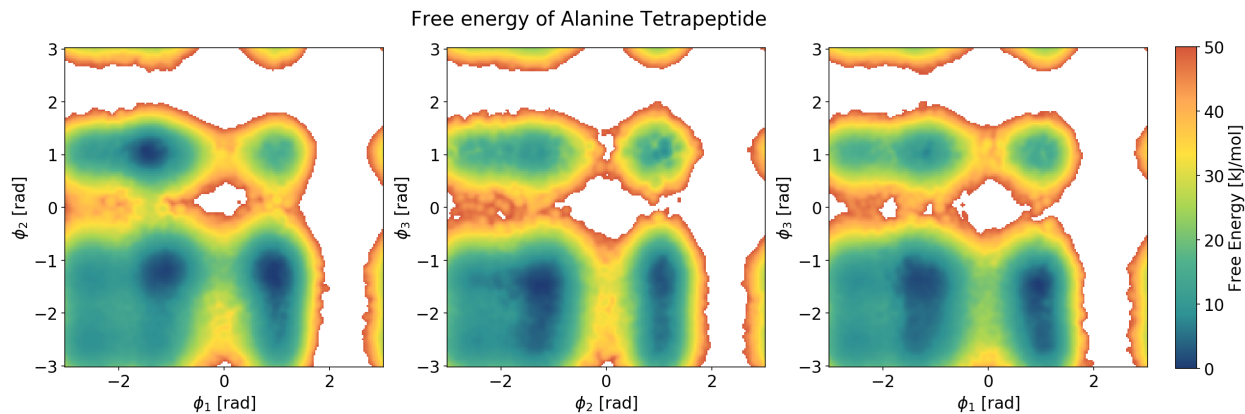


Figure 5: Two-dimensional free energy surfaces of Ala4 obtained with the reweighting, as a function of the three dihedral angles  $\{\phi_1, \phi_2, \phi_3\}$ .

this process. The crystallization and the melting process are marked by a local character. As a consequence, many CVs are defined in terms of per-atom crystallinity measures. Then the number of solid-like atoms is used as collective variable. In terms of these variables the free energy profile is characterized by very narrow minima, around 0 and  $N_{atoms}$ . In order to enhance in an efficient way the fluctuations in such space one often needs to employ variants of metadynamics [30] or an high order basis set expansion of the VES.

This can be easily addressed using the expressivity of neural networks, which we use here to represent rapidly varying features of the FES and to avoid boundaries artifacts. In figure 6 we show the free energy profile learnt by the NN as well the one recovered by reweighting. Even in the presence of very sharp boundaries, the NN bias is able to learn a good  $V_s$ , which allows for going back and forth efficiently between the two states and for recovering a good estimate of the FES in the subsequent reweight. The KL divergence threshold is reached in 10 ns, and the bias is no longer updated after 30ns.

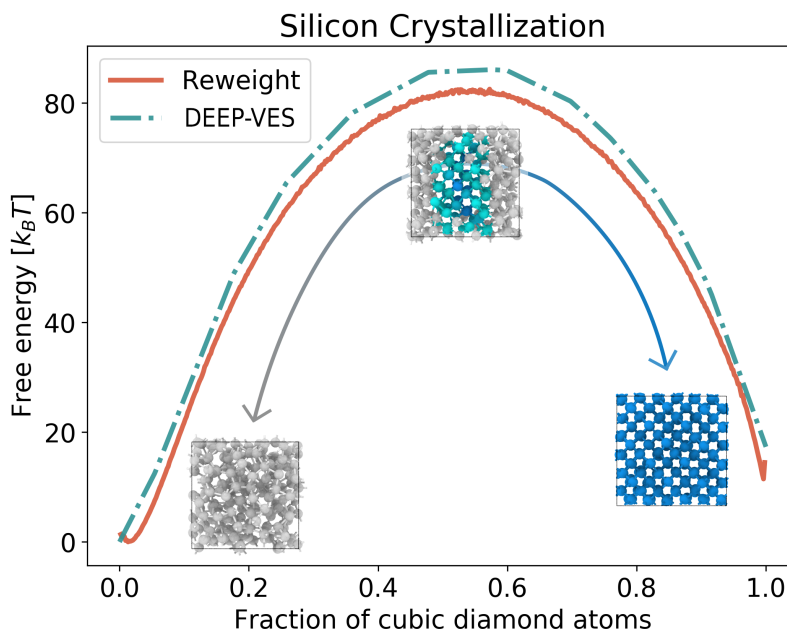


Figure 6: Free energy surface of silicon crystallization, in terms of the number of cubic diamonds atoms in the system. Snapshots of the two minima, as well as the transition state are also shown. The reweight is obtained using  $V_s$ . Regions of the FES greater than  $50 \text{ kJ/mol}$  are not shown.

### Choice of the parameters

After presenting the results, we would like to spend a few words on the choice of parameters. This procedure requires setting three parameters, namely the time scale for calculating the KL divergence, the KL threshold and the decay time for the learning rate. Our experience is that if the chosen set of CVs is good this choice has a limited impact on the simulation result. In the case of non-optimal CVs, more attention is required.

The KL divergence should be calculated on a time scale in which the system samples the target distribution, so the greater the relaxation time of the neglected variables, the greater this scale should be. However, this is only used to monitor convergence and therefore it is possible to choose a higher value without compromising speed. A similar argument applies to the decay constant of the learning rate, but in the spirit of reaching a constant potential quickly one tries to keep it lower (in the order of thousands of iterations). Finally, we found that the protocol is robust with respect to the epsilon parameter of the KL divergence threshold, provided that it is chosen in a range of values around 0.5. In the case of FES with larger dimensionality it may be appropriate to increase this parameter, in order to reach rapidly to a good estimate of  $V_s$ . In the supplementary information we report a study of the influence of these parameters in the accuracy of the bias learnt and the time needed to converge for the Wolfe-Quapp potential.

### Conclusions

In this work we have shown how the flexibility of neural networks can be used to represent the bias potential and the FES as well, in the context of the VES method. Using the same architecture and similar optimization parameters we were able to deal with different physical systems and FES dimensionalities. This include also the case in which some important degree of freedom is left out from the set of enhanced CVs. We plan to extend this to even higher dimensional landscapes, where the power of NNs can be fully exploited.

Our work is an example of a reinforcement learning scheme, where the neural network is optimized following a variational principle. Also the target distribution allows for an efficient sampling of the relevant configurational space, which is particularly important in the optics of sampling high dimensional FES.

In the process we have developed a minimization procedure alternative to that of ref. [14], which globally tempers the bias potential based on a Kullback Leibler divergence between the current and the target probability distribution. We think that also conventional VES can benefit from our new approach, and that we have made another step in the process of sampling complex free energy landscapes. Future goals might include developing a more efficient scheme to exploit the variational principle in the context of NNs, as well as learning not only the bias but also the collective variables on-the-fly. This work allows also tapping into the immense literature on machine learning and neural networks for the purpose of improving VES.

### Acknowledgements

This research was supported by the NCCR MARVEL, funded by the Swiss National Science Foundation, and European Union Grant No. ERC-2014-AdG-670227/VARMET. Calculations were carried out on the Euler cluster at ETH Zurich. The authors thank Michele Invernizzi for useful discussions and for carefully reading the paper.



## Materials and methods

The VES-NN is implemented on a private version of PLUMED2 [31], linked against LibTorch (PyTorch C++ library). The latter takes care of the construction and the optimization of the neural network. The gradients of the functional with respect to the parameters are computed inside PLUMED according to eq. 11. The first expectation value is computed by sampling, while the second is obtained by numerical integration over a grid. In the following we report the setup for the VES-NN and the simulations for all the examples reported in the paper.

### Wolfe-Quapp potential

The Wolfe-Quapp potential is a fourth-order polynomial:  $U(x, y) = x^4 + y^4 - 2x^2 - 4y^2 + xy + 0.3x + 0.1y$ . We rotated it by an angle  $\theta = -3/20 \pi$  in order to change the direction of the path connecting the two minima. A langevin dynamics is run with PLUMED using a timestep of 0.005, a target temperature of 1 and a friction parameter equal to 10 (in terms of natural units). The biasfactor for the well-tempered distribution is equal to 10. A neural network composed by [48,24,12] nodes is used to represent the bias. The learning rate is equal to 0.001. An optimization step of the NN is performed every 500 timesteps. The running KL divergence is computed on a timescale of  $5 \cdot 10^4$  iterations. The threshold is set to  $\epsilon = 0.5$  and the decay constant for the learning rate is set to  $5 \cdot 10^3$  iterations. The grid for computing the target distribution integrals has 100 bins. The parameters of the NN are the kept the same also for the following examples, unless otherwise stated.

### Peptides

For the Alanine dipeptide (Ace-Ala-Nme) and tetrapeptide (Ace-Ala3-Nme) simulations we use GROMACS [32] patched with PLUMED. The peptides are simulated in the NVT ensemble using the Amber99-SB force field [33] with a time step of 2 fs. The target temperature of 300K is controlled with the velocity rescaling thermostat [34]. The decay constant is chosen to be  $2 \cdot 10^3$  and the threshold is set to  $\epsilon = 0.5$  for Ala2 and to  $\epsilon = 1$ . for Ala4. For Ala2 a grid of 50x50 bins is used, while for Ala4 is composed by 20x20x20 bins. The biasfactor is equal to 10.

### Silicon

For the silicon simulations we use LAMMPS [35] patched with PLUMED, employing the Stillinger and Weber potential [36]. A 3x3x3 supercell (216 atoms) is simulated in the NPT ensemble with a timestep of 2 fs. The temperature of the thermostat [34] is set to 1700K with a relaxation time of 100 fs, while the values for the barostat [37] are 1 atm and 1 ps. The CV used is the number of cubic diamond atoms in the system, defined according to ref. [38]. The decay time for the learning rate is  $2 \cdot 10^3$ , and a grid of 216 bins is used. The biasfactor used is equal to 100.

## References

- [1] Jörg Behler and Michele Parrinello. Generalized neural-network representation of high-dimensional potential-energy surfaces. *Physical Review Letters*, 98(14):–, 2007.
- [2] Omar Valsson, Pratyush Tiwary, and Michele Parrinello. Enhancing Important Fluctuations: Rare Events and Metadynamics from a Conceptual Viewpoint. *Annu. Rev. Phys. Chem*, 67:159–84, 2016.
- [3] Wei Chen, Aik Rui Tan, and Andrew L Ferguson. Collective variable discovery and enhanced sampling using autoencoders: Innovations in network architecture and error function design. *Journal of Chemical Physics*, 149(7):72312, 2018.
- [4] Markus Schöberl, Nicholas Zabarar, and Phaedon-Stelios Koutsourelakis. Predictive Collective Variable Discovery with Deep Bayesian Models. 2018.
- [5] Carlos X. Hernández, Hannah K Wayment-Steele, Mohammad M Sultan, Brooke E Husic, and Vijay S Pande. Variational encoding of complex dynamics. *Physical Review E*, 97(6), 2018.
- [6] Christoph Wehmeyer and Frank Noé. Time-lagged autoencoders: Deep learning of slow collective variables for molecular kinetics. *Journal of Chemical Physics*, 148(24), 2018.
- [7] Dan Mendels, GiovanniMaria Piccini, and Michele Parrinello. Path collective variables without paths. 2018.
- [8] João Marcelo Lamim Ribeiro, Pablo Bravo, Yihang Wang, and Pratyush Tiwary. Reweighted autoencoded variational Bayes for enhanced sampling (RAVE). *Journal of Chemical Physics*, 149(7):1–10, 2018.
- [9] Letif Mones, Noam Bernstein, and Gábor Csányi. Exploration, Sampling, and Reconstruction of Free Energy Surfaces with Gaussian Process Regression. *Journal of Chemical Theory and Computation*, 12(10):5100–5110, 2016.
- [10] Raimondas Galvelis and Yuji Sugita. Neural Network and Nearest Neighbor Algorithms for Enhancing Sampling of Molecular Dynamics. *Journal of Chemical Theory and Computation*, 13(6):2489–2500, 2017.
- [11] Hythem Sidky and Jonathan K Whitmer. Learning free energy landscapes using artificial neural networks. *Journal of Chemical Physics*, 148(10):104111, 2018.
- [12] Linfeng Zhang, Han Wang, and E. Weinan. Reinforced dynamics for enhanced sampling in large atomic and molecular systems. *Journal of Chemical Physics*, 148(12), 2018.
- [13] Luigi Bonati and Michele Parrinello. Silicon liquid structure and crystal nucleation from ab-initio deep Metadynamics. *Physical Review Letters*, 121, 2018.
- [14] Omar Valsson and Michele Parrinello. Variational approach to enhanced sampling and free energy calculations. *Physical Review Letters*, 113(9), 2014.
- [15] Michele Invernizzi, Omar Valsson, and Michele Parrinello. Coarse graining from variationally enhanced sampling applied to the Ginzburg–Landau model. *Proceedings of the National Academy of Sciences*, 114(13):3370–3374, 2017.
- [16] Omar Valsson and Michele Parrinello. Well-tempered variational approach to enhanced sampling. *Journal of Chemical Theory and Computation*, 11(5):1996–2002, 2015.
- [17] James McCarty, Omar Valsson, Pratyush Tiwary, and Michele Parrinello. Variationally Optimized Free-Energy Flooding for Rate Calculation. *Physical Review Letters*, 115(7), 2015.
- [18] Pablo M. Piaggi, Omar Valsson, and Michele Parrinello. A variational approach to nucleation simulation. *Faraday Discuss.*, 195:557–568, 2016.
- [19] Pablo M Piaggi and Michele Parrinello. Multithermal-Multibaric Molecular Simulations from a Variational Principle. 2019.
- [20] James McCarty, Omar Valsson, and Michele Parrinello. Bespoke Bias for Obtaining Free Energy Differences within Variationally Enhanced Sampling. *Journal of Chemical Theory and Computation*, 12(5):2162–2169, 2016.
- [21] Michele Invernizzi and Michele Parrinello. Making the best of a bad situation: a multiscale approach to free energy calculation. *Journal of Chemical Theory and Computation*, 2019.
- [22] Ian Goodfellow, Yoshua Bengio, and Aaron Courville. *Deep Learning*. MIT Press, 2016.
- [23] G. M. Torrie and J. P. Valleau. Nonphysical sampling distributions in Monte Carlo free-energy estimation: Umbrella sampling. *Journal of Computational Physics*, 23(2):187–199, 1977.
- [24] Alessandro Laio and Michele Parrinello. Escaping Free-Energy Minima. *Proc. Natl. Acad. Sci. U. S. A.*, 99:12562, 2002.

- [25] Patrick Shaffer, Omar Valsson, and Michele Parrinello. Enhanced, targeted sampling of high-dimensional free-energy landscapes using variationally enhanced sampling, with an application to chignolin. *Proceedings of the National Academy of Sciences*, 113(5):1150–1155, 2016.
- [26] Alessandro Barducci, Giovanni Bussi, and Michele Parrinello. Well-tempered metadynamics: A smoothly converging and tunable free-energy method. *Physical Review Letters*, 100(2):–, 2008.
- [27] Yann A. LeCun, Léon Bottou, Genevieve B. Orr, and Klaus Robert Müller. Efficient backprop. *Lecture Notes in Computer Science*, 7700:9–48, 2012.
- [28] Francis Bach and Eric Moulines. Non-strongly-convex smooth stochastic approximation with convergence rate  $O(1/n)$ . 2013.
- [29] Diederik P Kingma and Jimmy Ba. Adam: A Method for Stochastic Optimization. 2014.
- [30] Davide Branduardi, Giovanni Bussi, and Michele Parrinello. Metadynamics with adaptive gaussians. *Journal of Chemical Theory and Computation*, 8(7):2247–2254, 2012.
- [31] Gareth A Tribello, Massimiliano Bonomi, Davide Branduardi, Carlo Camilloni, and Giovanni Bussi. PLUMED 2: New feathers for an old bird. *Computer Physics Communications*, 185(2):604–613, 2014.
- [32] David Van Der Spoel, Erik Lindahl, Berk Hess, Gerrit Groenhof, Alan E. Mark, and Herman J.C. Berendsen. GROMACS: Fast, flexible, and free, 2005.
- [33] Viktor Hornak, Robert Abel, Asim Okur, Bentley Strockbine, Adrian Roitberg, and Carlos Simmerling. Comparison of multiple amber force fields and development of improved protein backbone parameters, 2006.
- [34] Giovanni Bussi, Davide Donadio, and Michele Parrinello. Canonical sampling through velocity rescaling. *The Journal of chemical physics*, 126(1):14101, 2007.
- [35] S Plimpton. LAMMPS-large-scale atomic/molecular massively parallel simulator. *Sandia National Laboratories*, pages –, 2007.
- [36] Frank H. Stillinger and Thomas A. Weber. Computer simulation of local order in condensed phases of silicon. *Physical Review B*, 31(8):5262–5271, 1985.
- [37] Glenn J. Martyna, Douglas J. Tobias, and Michael L. Klein. Constant pressure molecular dynamics algorithms. *The Journal of Chemical Physics*, 101(5):4177–4189, 1994.
- [38] Pablo Piaggi and Michele Parrinello. *To be published.*